Acta Cryst. (1967). **22**, 14

Electron Diffraction Study of MgO *h*00-systematic Interactions

BY P. GOODMAN

Division of Chemical Physics, C.S.I.R.O. Chemical Research Laboratories, Melbourne, Australia

AND G. LEHMPFUHL

Fritz-Haber-Institut der Max-Planck-Gesellschaft, Berlin-Dahlem, Germany

(*Received* 21 *June* 1966)

An investigation was made of the MgO *h*00-systematic interactions using the experimental method of fine-focus convergent beam electron diffraction. The experimental data were compared directly with intensity distributions computed from assumed MgO structure factors by multiple-beam diffraction theory.

The investigation showed that close agreement could be obtained between calculation and experiment provided specific values were chosen for the scattering potentials and the crystal thickness. Close agreement was found with a value of $V_{200}=6{\cdot}92$ volt. This value is appreciably lower than the value of 7·29 volt derived from the Hartree–Fock calculations for neutral atoms, but is in agreement with the scattering curve derived by Tokonami using a model for the O^{2-} ion recently developed by Yamashita.

A form of distribution was found for the absorbing potential (leading to a Borrmann effect) which was close to that of δ functions located at the atom sites. The value obtained for V'_{200}, 0·14 volt, was considerably lower than that estimated in some earlier investigations. Experimental and theoretical reasons for this difference are given. It was apparent that study of a more strongly interacting reflexion set than the MgO *h*00-systematics would give more precision in the potential determination. In fitting the calculated and experimental curves the crystal thickness was determined to within one unit cell or with an accuracy of 0·5 % for the crystals studied.

Introduction

Many studies have been made in the past of dynamic effects in diffraction patterns from magnesium oxide. Recently single wedge-crystals have been examined, both in a diffraction camera (Lehmpfuhl & Molière, 1961, 1962), and in the electron microscope (Kamiya, 1963; Uyeda & Nonoyama, 1965) to obtain values of V_h and V'_h, the Fourier coefficients of the elastic and inelastic scattering potential. Mostly the two-beam approximation of Bethe has been used for these determinations.

From the magnitude of the term (V_g/g^2) implicit in Bethe's derivation for addition-potentials, the importance of the higher order interferences can be estimated in each case. It is expected that this systematic interference effect will be more important for the 200 reflexion than for example for the 220 and 420 reflexions. Estimates made for V_{200} and V'_{200} from the two-beam calculation will be in error from this effect. Corrections for the weak beams in the form of addition-potentials can be applied from Bethe's theory under certain conditions, namely when the excitation error for the main beam is very small and the excitation errors of all other reflexions appearing in the correction terms are large. However, this correction gives no solution for the weak beams, nor for the main beams far from the Bragg position. On the other hand as has been pointed out by Howie & Whelan (1960), when *n*-beam theory is used the systematic effect itself can lead to a better determination of the scattering potentials, and in particular of the absorption factors, provided the experimental data are adequate.

MacGillavry (1940) showed that the method of convergent beam diffraction due to Kossel & Möllenstedt (1942) could be used to estimate structure potentials, by assuming the two-beam approximation. Ackermann (1948), in extending the convergent beam investigation to several substances, showed the limitations of the two-beam approximation when applied to quantitative work. More general application of this experimental method has since been prevented by the requirement of the original technique for large perfect crystal plates, and further by the lack of a practical method of accurate interpretation.

A recent refinement of Möllenstedt's method using improved optics enables diffraction patterns to be obtained from very small regions of about 300 Å diameter (Goodman & Lehmpfuhl, 1965), which are generally perfect and of constant thickness, and data of this type are suitable for quantitative analysis. The patterns obtained, particularly for the weak beams, generally show very complicated intensity distributions unlike the two-beam formulation. In comparing such a distribution with one derived by a suitable calculation we have many separate points of comparison, so that one pattern may give sufficient information for a determination of several scattering potentials. The multiple-slice calculation for *n*-beam diffraction (Cowley & Moodie, 1957) provides a suitable method for obtaining calculated angular intensity distributions (Goodman & Moodie, 1966). By this procedure the intensities are

computed at fine intervals of crystal thickness, allowing an accurate determination of this parameter to be made by a direct comparison with experiment. The original multiple-slice formulation above was corrected to give the relativistic form, in the manner suggested by Fujiwara (1961) (see *Discussion*), and all references to this calculation imply this corrected form.

The purpose of the present investigation was to test the accuracy of the calculation procedure, and further to investigate the sensitivity of *n*-beam intensity distributions to the values of the structure potentials.

Experimental

To obtain quantitative results from convergent beam experiments it is necessary to use crystals of uniform thickness, as integration over a small thickness range can change the apparent shape of the intensity distribution. Suitable conditions were found for collecting thin perfect plates of magnesium oxide grown in (100) orientation, from magnesium ribbon burned in air (Fig. 1). The crystals were collected on a specimen grid covered with carbon film, which was mounted in the Valdré tilt holder of a new diffraction apparatus (Cockayne, Goodman, Mills & Moodie, 1966). The volume surrounding the specimen was cooled by liquid nitrogen to reduce contamination, the cold surface being formed by a cold cap containing an aperture above the specimen, and a cold divergent funnel below the Valdré holder. The crystals were brought into a suitable orientation for obtaining the *h*00 line of diffraction without serious disturbance from other reflexions, and pictures were taken of the 200 and 400 excitations from crystals of different thickness using an accelerating voltage of 79·45 kV. The pictures were recorded on Ilford N4·50 70 mm film, which was found to have good linearity for blackening over the range used for the experiment. The film was first calibrated, and a series of diffraction pictures taken with accurately known exposure times by means of an electronic shutter. The pictures used for the weak beam investigation were taken with an exposure eight times that used for the strong beam pictures (Fig. 3).

Conditions for one-dimensional diffraction

In order to obtain results sufficiently rapidly and simply, the calculations were performed only for the systematic case, *i.e.* considering only interactions arising from the *h*00 reflexion set. This constitutes a one-dimensional calculation. With a simple light atom structure such as magnesium oxide it is possible to find orientations sufficiently far from a two-dimensional diffraction position to avoid strong extra interferences.

The patterns used are shown in Fig. 3. It can be seen that the main structure of the intensity distribution is one-dimensional, and that the weak crossing lines which occur appear to have little perturbing effect on the pattern. The accuracy of the one-dimensional calculation was tested by comparison of the results with the experimental distribution from these patterns. Detailed agreement was obtained (Figs. 6 and 8), and this calculation was adopted for the present investigation.

In general the applicability of the systematic approximation may be tested experimentally and with calculation. Experimentally it may be seen if the measured quantity, such as V_h or V_h' in the present case, changes when different regions of the pattern are used, as for example on either side of a crossing weak interaction. By calculation the results of a two-dimensional calculation for different chosen orientations can be compared directly with the results of the one-dimensional calculation.

Apart from the small differences which may be detected in this way certain types of marked deviation from the ideal one-dimensional case have been noted. Firstly in the neighbourhood of a strong zone axis where reflexions having large structure factors and large excitation errors begin to disturb the intensities, the bands in the pattern become noticeably nonparallel. This effect is seen clearly in Fig. 2 showing the MgO 220 reflexion taken near a zone axis. Since the intensities are changing rapidly with crystal orientation in a non-systematic direction, these cases are not suitable for simple interpretation.

Secondly cases are observed where the convergent beam pattern retains its one-dimensional structure, *i.e.* with parallel bands, but is affected uniformly by neighbouring interactions. An illustration of such a case is provided by the cadmium sulphide Kossel pattern taken around the $41\bar{5}0$ zone axis published elsewhere (Goodman & Lehmpfuhl, 1966). In such cases corresponding to a zone axis of low order, it may be sufficient to use a one-dimensional calculation but using 'corrected' Fourier scattering coefficients (*e.g.* coefficients obtained by a two-dimensional phase grating or other thin crystal calculation).

Finally regions of strong interaction such as a principal zone axis have already been shown to be useful for examining crystal symmetries by qualitative methods (Goodman & Lehmpfuhl, 1966). For a quantitative analysis such pictures require full two-dimensional calculation. For the present exploratory study these orientations offered no advantage. In fact the one-dimensional study allows comparison of the scattering and absorption coefficients measured specifically along certain crystal directions. However, it is expected that two-dimensional examinations of other special orientations will be valuable.

Analysis

The systematic calculation used in this investigation included interactions between 13 beams. The behaviour of four of these beams – zero beam, main diffracted beam and the next two strongest beams – was studied. As seen below the two strong beam distributions contained the most definite information about the struc-

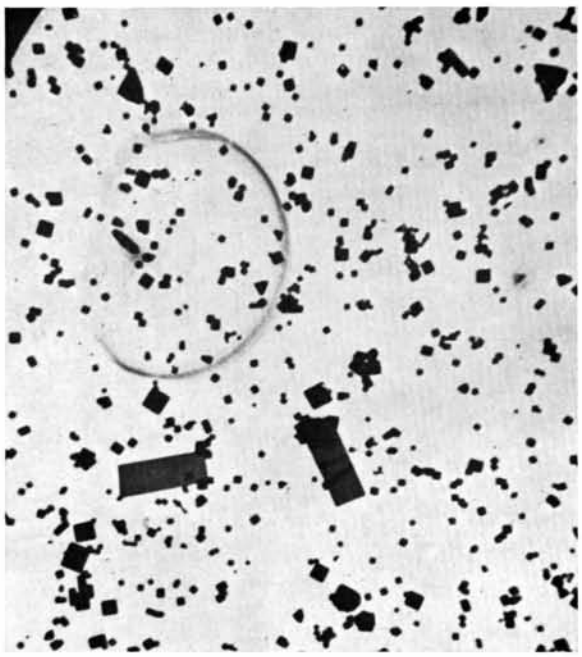

Fig. 1. Shadow micrograph taken in convergent-beam apparatus, showing region of magnesium oxide smoke with cube and plate crystals. Long edge of plates is ~1·0 micron.

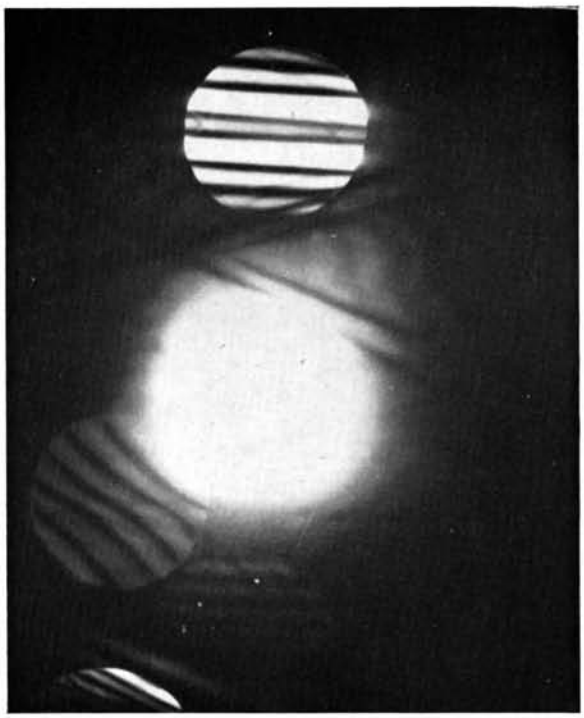

Fig. 2. Pattern from magnesium oxide 220 reflexion, showing the effect of neighbouring region of strong interaction. Fringe separation decreases towards the zone axis which is just beyond the right-hand edge of the photograph.

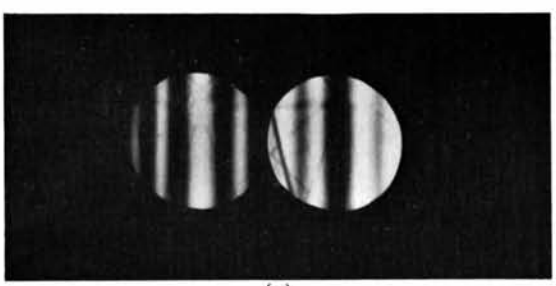

(*a*)

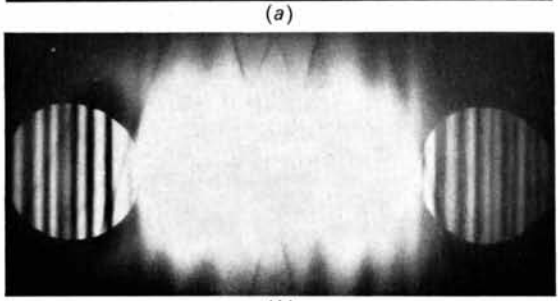

(*b*)

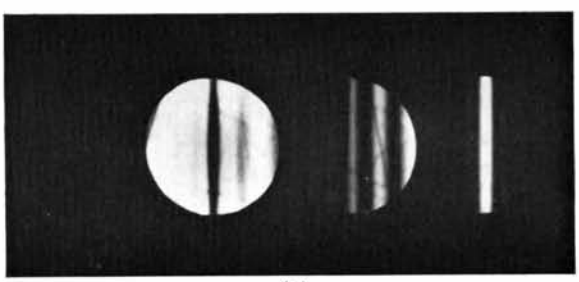

(*c*)

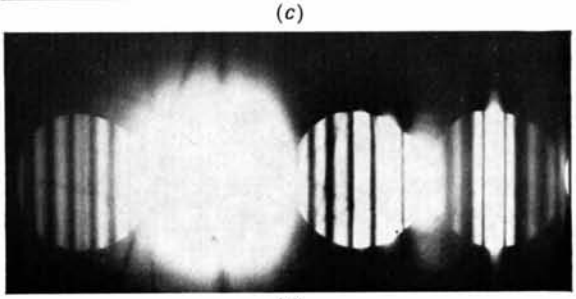

(*d*)

Fig. 3. Convergent beam pattern from plate crystal, showing 200 and 400 excitation. (*a*) 200 excitation, strong beams, 0·2 sec exposure. (*b*) 200 excitation, weak beams, 1·6 sec exposure. (*c*) 400 excitation, strong beams, 0·2 sec exposure. (*d*) 400 excitation, weak beams, 1·6 sec exposure.

[*To face p.* 15

ture potentials examined, and the weak beam distributions determined the crystal thickness. The structure potentials ($V_h + iV_h'$) were used as input to the calculation. A set of six independent structure potentials was used. Only the first two structure potentials V_{200} and V_{400} were refined, and of those V_{200} was determined with the greater accuracy. The *n*-beam calculation was not sufficiently sensitive to permit refinement of higher order values of V_h. Since however these values refer to the outer part of the scattering curve they are of less interest.

The two cases of excitation of the 200 and of the 400 reflexion were analysed.

200 *Excitation – non-absorbing scattering*

Pictures were taken with the diffraction aperture adjusted symmetrically about the 200 Bragg position with two different exposures [Fig. 3(*a*) and (*b*)].

A corresponding relativistically corrected calculation was made by the multi-slice method, at first with a non-absorbing potential. This could be fitted to the experimental curves for the diffracted beams, since the main effect of absorption is found in the zero beam distribution. An approximate value for the crystal thickness was first obtained by examining the spacing of subsidiary maxima in one or two isolated weak diffraction spots. Then by comparing the calculated intensity distributions in this thickness region with the experimental curves for the two weaker beams, in this case the 400 and $\bar{2}00$ reflexions, a more exact value was obtained for the thickness. Since these beams have a more rapidly oscillating distribution than the strong (000, 200) beams, the experimental curves generally will fit for only one value of thickness. The fit at this stage was not perfect because of the values chosen for the main structure factors. In this diffraction pattern the 200 distribution gives the most direct guide to the 200 structure potential. A discrepancy was observed between the positions of the minima in the calculated and experimental 200 distributions. A correction for the value of V_{200} was estimated which would bring the calculated distribution into agreement. Now a perfect fit was possible with a thickness perhaps one or two unit cells away from the previous estimate. In this way the crystal thickness was determined to within one unit cell (4·2 Å).

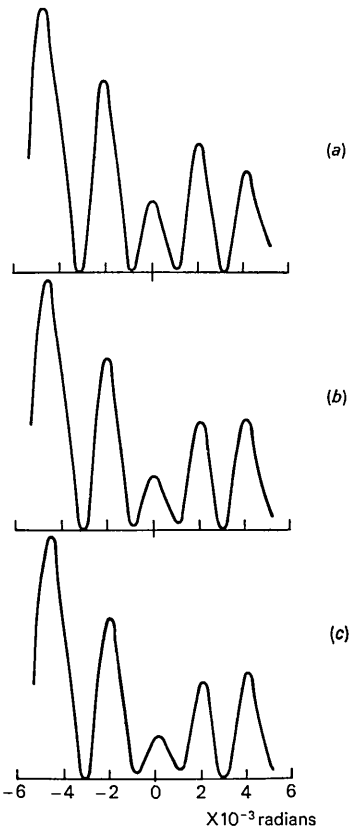

Fig. 5. Calculated intensity distribution of the $\bar{2}00$ reflexion with 200 excitation for changing V_{200}. (*a*) $V_{200} = 7{\cdot}24$ volt, $n = 158$. (*b*) $V_{200} = 6{\cdot}79$ volt, $n = 159$. (*c*) $V_{200} = 6{\cdot}92$ volt, $n = 159$. The value n is chosen for closest agreement between distributions.

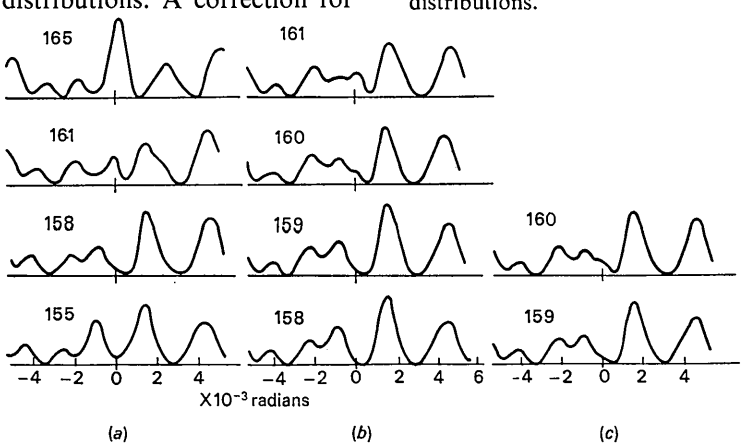

Fig. 4. Calculated intensity distributions of the 400 reflexion with 200 excitation, corresponding to different values of V_{200} and crystal thickness n, expressed in units of 4·2 Å. The value of n is shown to the left of each curve. (*a*) $V_{200} = 7{\cdot}23$ volt. (Corresponding approximately to the Hartree–Fock neutral atom value). (*b*) $V_{200} = 7{\cdot}79$ volt. (*c*) $V_{200} = 6{\cdot}92$ volt. Distributions are arranged in decreasing thickness from the top in each column, and values of n are chosen to give best agreement between the distributions in the same row.

The sensitivity of the calculated weak beam distributions to changing values of V_{200} and thickness is shown in Figs. 4 and 5. The behaviour of the 400 reflexion seen in Fig. 4 shows that these parameters cannot be independently determined from this reflexion alone, but if V_{200} is known from another reflexion, the thickness can be determined accurately. Fig. 5 shows the sensitivity of the $\bar{2}00$ to the V_{200} value; for this reflexion the intensity features show a more definite dependence on this value. The 200 distribution calculated for the correct thickness was finally compared with experiment to check if any detectable error remained in the value arrived at for V_{200}. From this analysis, using only elastic scattering calculations together with the experimental distributions from the diffracted beams, the value $V_h = 6{\cdot}92 \pm 0{\cdot}07$ volt was obtained.

Scattering with absorption

The analysis with a non-absorbing potential fails to account for the asymmetry in the 000 beam distribution. It was shown by Hashimoto, Howie & Whelan (1962) that this asymmetry could be explained in the two-beam approximation by using a complex potential $(V_h + iV_h^i)$ to introduce a phenomenological absorption coefficient. This method was further used by Howie & Whelan (1960) in a many-beam calculation to examine the absorption effect for aluminum.

By now adding an imaginary term V_h^i to the real part of the structure potentials already determined in the above analysis, the intensity distributions were recalculated. The only appreciable change occurred in the 000 distribution where an asymmetry was introduced. At first values were given to V_h^i assuming the relation

$$V_h^i = \text{constant} \,.\, V_h \,. \qquad (1)$$

With this inelastic scattering curve, of the same shape as the elastic one, it was possible to fit the 000 experimental distribution exactly by choosing a certain ratio for V_h^i/V_h. The resulting values for the first three of the V_h^i, were:

$$V_{200}^i = 0{\cdot}16 \text{ volt.} \quad V_{400}^i = 0{\cdot}07 \text{ volt.} \quad V_{600}^i = 0{\cdot}04 \text{ volt.}$$

At this point all four experimental beam distributions were fitted by the calculated values, and the addition of the imaginary potential did not change the previous estimate for the crystal thickness and the V_h set.

A second model for the inelastic potential was then taken, namely:

$$V_h^i = \text{constant} \,, \qquad (2)$$

which is equivalent to a distribution in the crystal of a set of δ functions located at the atom sites. It was also found possible to fit the 000 distribution with this model, using a value for V_h^i of 0·14 volt.

The form of the absorption scattering curve could thus not be determined from the study of the 200 excitation alone. The resulting final agreement is shown in Fig. 6, where the calculated and experimental curves for the four beams are shown, for the pattern of Fig. 3(*a*) and (*b*).

400 excitation

Fig. 3(*c*) and (*d*) shows two exposures of the pattern obtained with the 400 reflexion excited. Using the values for thickness and V_h determined in the previous case calculations were made, at first for non-absorbing scattering, in order to study the four beams, $\bar{2}00$, 000, 200 and 400. All the experimental beam distributions, excluding the 000, were again well described by these values.* It will be noted that the calculated 000 beam distribution shows an asymmetry using only a non-absorbing potential [Fig. 7(*a*)]. This is the 'absorption' effect due to weak beams (Gjønnes, 1961).

The two models given in the last section for the V_h^i set of absorbing potential coefficients were then used in the calculation. The first model (1) gave a 000 distribution with almost no asymmetry [Fig. 7(*b*)], while the second model (2) [Fig. 7(*c*)] gave an asymmetry very close to the experimental curve. It was therefore possible from a study of the 400 case to distinguish between these two models. This is in agreement with the observation of Howie & Whelan (1960) for aluminum,

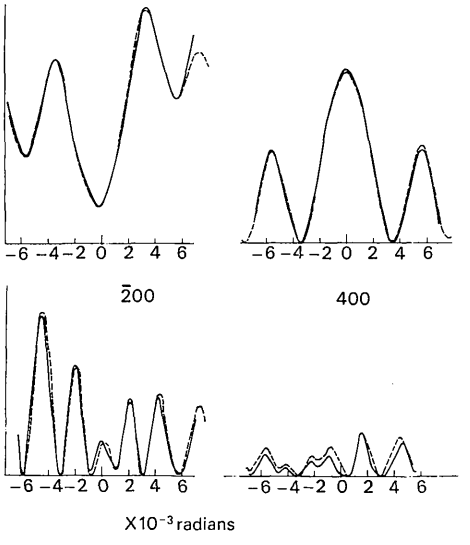

Fig. 6. Experimental and calculated intensity distribution for the 000, 200, $\bar{2}00$, 400 reflexions, with the 200 beam excited. Experimental curves, shown as a broken line, are obtained by microphotometer recording from diagrams of Fig. 3(*a*) and (*b*). The full curves are calculated assuming $V_{200} = 6{\cdot}92$ volt, $V_h^i = 0{\cdot}14$ volt, and a crystal thickness of 159 unit cells.

* In this analysis the thickness obtained in the 200 study was 159 unit cells and in the 400 study 160 unit cells. The method is sufficiently sensitive to distinguish between these two values. Since by moving the diffraction aperture during the experiment from the 200 reflexion to obtain the 400 reflexion the focused beam must move on the crystal, it is possible that this difference corresponds to a single unit-cell step on the crystal surface.

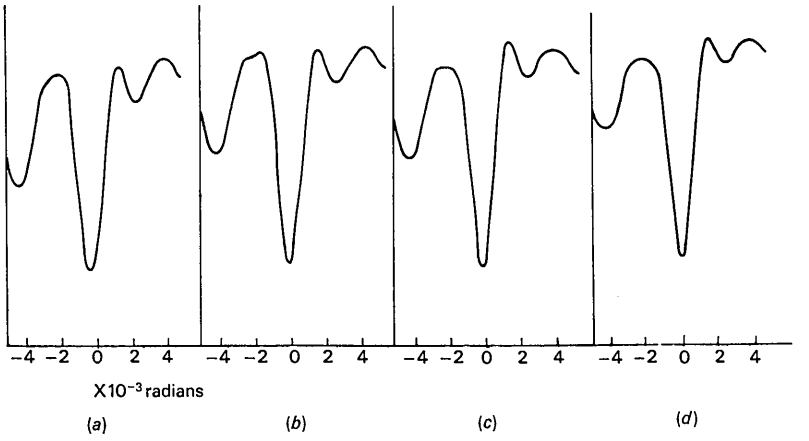

Fig. 7. Calculated and experimental intensity distributions for the 000 reflexion with 400 excitation. (*a*) Calculated, with no absorption. (*b*) Calculated, with V_h^i proportional to V_h. (*c*) Calculated, with $V_h^i = 0{\cdot}14$ volt, independant of h. (*d*) Experimental distribution.

that with systematic interaction the higher order reflexion cases show greater sensitivity in the 000 distribution to the nature of the absorption potential. The third order 600 was not studied; the lesser degree of interaction in the magnesium oxide case made this excitation less valuable.

The final agreement obtained between calculation and experiment for this case is shown in Fig. 8. From this study it was found that the intensity distribution could be fully explained by assuming an absorption distribution given by a set of δ functions with Fourier coefficients of approximately 0·14 volt.

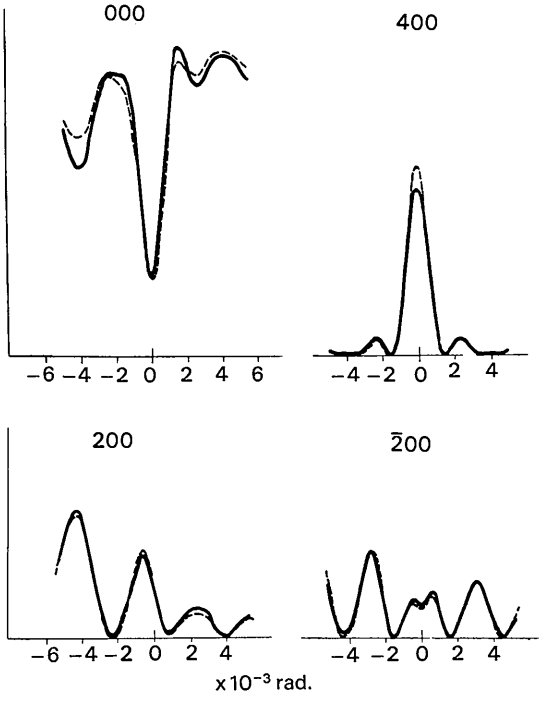

Fig. 8. Experimental and calculated intensity distributions for the 000, 400, 200, $\bar{2}00$ reflexions, with the 400 beam excited. Experimental curves shown as a broken line are obtained from diagrams of Fig. 3(*c*) and (*d*). Full curves are calculated with values as in Fig. 6.

Discussion

I. V_h determination

Comparison with other experimental results

The electron diffraction values previously obtained for magnesium oxide structure potentials show a wide spread, partly due to neglecting important effects in the interpretation, namely, the influence of weak beams and an incorrect application of the relativistic effect. On the latter point Fujiwara (1961) has shown that the introduction of the relativistic wavelength $\lambda = h\{2m_0Ee(1+eE/2m_0c^2)\}^{-\frac{1}{2}}$ (where E is the accelerating voltage for the electrons) into the scattering equations is not sufficient, but that it is also necessary to introduce the relativistic mass, $m = m_0(1-\beta^2)^{-\frac{1}{2}}$. The two terms occur together as $\frac{1}{2}\{1+(1-\beta^2)^{\frac{1}{2}}\}$ in the two beam approximation and the phase-grating theory. Fujiwara's correction is significant for $E = 80$ kV. (See also Miyake, Fujiwara & Suzuki, 1963).

The relative importance of the weak beam effect in different cases has been discussed in the *Introduction*. Even when this effect is small for a particular diffraction pattern its omission can cause difficulties when the excitation error or accelerating voltage are changed. As is now understood from *n*-beam calculations, its influence does not go to zero at large thickness, as was assumed by Hashimoto (1964), and its increasing importance at high voltages is seen in the extinction length anomaly reported by Dupouy, Perrier, Uyeda & Ayroles (1965). The magnitudes of this effect and of the relativistic corrections for the 200 reflexion may be estimated from the present calculation in the following way: With an accelerating voltage of 79·45 kV and a structure potential $V_{200} = 6{\cdot}92$ volt the extinction length as determined from the *n*-beam results computed as a function of thickness, for the case of zero excita-

tion error, is $1_{200}=408$ Å.* Substituting this value in the relativistically corrected two-beam formula,

$$V'_h=\frac{1}{\lambda l_h}\cdot\frac{h^2}{2m_0e}(1-\beta^2)^{\frac{1}{2}}=\frac{E\lambda}{l_h}\cdot\frac{1}{2}\{1+(1-\beta^2)^{\frac{1}{2}}\}$$

we obtain a 'structure potential' of 7·61 volts. The two-beam formula uncorrected for relativistic effects, namely:

$$V''_h=\frac{1}{\lambda l_h}\cdot\frac{h^2}{2m_0e}$$

with the same substitution gives a value of 8·8 volts. The systematic interferences in this case reduce the two-beam estimate of V_h by 10%, and the relativistic correction of V_h is of the same order of magnitude. Table 1 shows the V_{200} data obtained in other investigations from different measurements and using different methods of interpretation. When the appropriate corrections are applied the measurements show improved agreement with the present value. After correcting for relativity (references *A* to *D* of Table 1), the Bethe correction calculated for the $(400-\bar{2}00)$ effect with the excitation error $\zeta_{200}=0$ was applied when appropriate (*B*, *E*). Early references (*A* to *C*) refer to measurements made on single fine structure patterns found in powder ring patterns. A weak beam correction could not be applied in *A* and *C*, because non-zero values of excitation error were used; in *C* observed values show a strong dependence on excitation error (Wagenfeld, 1958).

* If the extinction length is measured from the *n*-beam calculated results, for *h*00 exactly satisfied, the lengths measured for the 000 and *h*00 are different. This is illustrated in Fig. 9 showing the 000 and 200 beam distributions in the hundred unit cells region. The perturbation of the 000 beam distribution near the extinction distance due to higher order interferences is clearly seen. If the cosine distribution is continued into this region, as shown by the broken line, the same extinction length may be obtained from both distributions. This is the definition of the extinction length used in the above calculation.

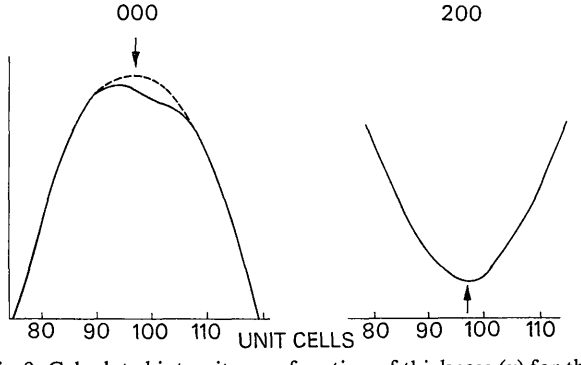

Fig. 9. Calculated intensity as a function of thickness (*n*) for the 000, 200 beams, with exact 200 excitation, near the region of extinction. Broken curve shows a cosine distribution for the 000 intensity.

Comparison with theory

The present value of V_{200} may be compared with values from theoretically derived scattering curves. Calculation of a scattering curve for the magnesium oxide structure is complicated by the difficulty of obtaining a model for the O^{2-} ion. The scattering curve for the Mg^{2+} ion differs little from that of the neutral atom in this region, so that the scattering factor is mainly sensitive to the O^{2-} model. Recent theoretical treatments of O^{2-} lead to results for V_{200} sufficiently divergent to be examined with the present experimental accuracy.

A recent scattering curve calculation by Tokonami (1966) makes use of the improved O^{2-} wave functions derived by Yamashita for the magnesium oxide structure. Yamashita's derivation (as reported by Togawa, 1965), incorporates the model for the outer $2p$ electrons placed in the Mg^{2+} field of MgO as in his earlier calculation (Yamashita & Kojima, 1952), but in addition uses the Watson wave functions for the $1s$ and $2s$ electrons placed in a $+1$ potential well (Watson, 1958), instead of assuming these wave functions as given for the free O^- ion, as in the first calculation. Tokonami's result shows appreciable differences from the earlier calculations of Suzuki (1960) for an O^{2-} ion in a $+1$ and $+2$ well, and from calculations made for the neutral atom, at the 200 scattering angle. These values are shown in Table 2(*a*).

The electron diffraction measurement appears at present more suitable for comparison with theory than the X-ray results, which are complicated for example

Table 1. *Values for V_{200} in volts from other experiments*

The second value (column 4) has been corrected where necessary for the relativistic effect, and for weak beam effects (using Bethe's addition-potential for the 400–$\bar{2}$00 interaction). Suffixes (1) and (2) indicate the value uncorrected for weak beams and relativity respectively.

Reference	Authors	Reported value	Corrected value	Comments
A	Molière & Niehrs (1955)	$7{\cdot}55^{(1),(2)}$	$(7{\cdot}17^{(1)})$	Average from 21 patterns, with different small ζ values.
B	Cowley, Goodman & Rees (1957)	$8{\cdot}0^{(1),(2)}$	7·0	Average from several patterns, for $\zeta\sim0$.
C	Molière & Wagenfeld (1958)	$7{\cdot}57^{(1),(2)}$	$(7{\cdot}15^{(1)})$	One pattern, different voltages, ζ calculated.
D	Lehmpfuhl & Molière (1961)	$7{\cdot}7^{(2)}$	7·3	One pattern. Bethe's correction included.
E	Uyeda & Nonoyama (1965)	$7{\cdot}46^{(1)}$	6·7	Systematic case only.
	Present analysis		6·92	

Table 2. *V_{200} in volts derived from theoretical (a), and from experimental (b) values for the O^{2-} scattering factor, together with the present electron diffraction measurement, and also the theoretical value for neutral* (Mg+O)

Value assumed for $F_x Mg^{2+}$ (except for the 1st and 7th tabulation) is 8·31.

	(*a*)	
A	Neutral atoms	7·40 volt
B	Suzuki–Watson (1*s*, 2*s*, 2*p*; +1 well)	7·27
C	Suzuki–Watson (1*s*, 2*s*, 2*p*; +2 well)	7·17
D	*Tokonami–Yamashita (1*s*, 2*s*; +1 well; 2*p*, Mg^{2+} potential)	7·01
	(*b*)	
	†Togawa (experimental $F_x O^{2-}$)	6·90 volt
	†Burley (experimental $F_x O^{2-}$)	7·12
	‡Present experiment (temperature corrected)	7·02

* Value obtained from published curve (Fig. 3 of reference).

† Values estimated using the experimental values given for O^{2-} and the fixed theoretical values for Mg^{2+} to allow a comparison with other results. The value given for Togawa was obtained by interpolation. If the experimentally obtained values for Mg^{2+} were used these values would be lower.

‡ Temperature factor $B=0{\cdot}26$ was assumed. At this stage no attempt has been made to determine B from the experiment. However, for this reflexion the result is insensitive to B.

by scaling factors, orientation in the powder samples, and undetermined extinction effects. (However the possibility of accurate X-ray measurements has been demonstrated by Hattori, Kuriyama, Katagawa & Kato, 1963). Two recent X-ray measurements have been made on magnesium oxide, but the results are not in agreement. Togawa (1965), using magnesium oxide powder obtained by burning magnesium in air, found agreement with the theoretical Tokonami curve. On the other hand, Burley (1965), measuring the X-ray scattering from a powder sample obtained by thermal decomposition of magnesium carbonate, gave a lower value for the structure factor in apparent agreement with Suzuki's +2 potential well calculation. The disagreement of the two experiments possibly arises from the different methods of preparation, or from a combination of this and different methods of interpretation.

The experimental V_{200} values are shown in Table 2(*b*), and may be compared with those predicted by theory shown in Table 2(*a*).

The present value of $V_{200}=7{\cdot}02$ volt (temperature corrected for 0 °K) agrees well with Tokonami's result.* However, since this represents only one point in the scattering curve it is valuable to compare results for another reflexion, particularly for the 111, which lies in the interesting low angle region, and unlike the 200 involves the difference of the two atomic scattering factors. For the 111 excitation the two-beam approximation is always in error owing to the influence of the 222 reflexion. For this reason most early electron diffraction measurements of V_{111} are in error. It is not possible in this case to make a correction by use of addition potentials. Molière & Wagenfeld (1957) studied the simultaneous reflexion of the 111 and 222 beams by measurements of the diffraction fine-structure, and by solving the dispersion equations (Bethe), assuming a three-beam case. The three-beam approximation has good accuracy for some orientations with 111 excitation owing to the large value of V_{222} compared with V_{111} and V_{333}.

The result obtained for V_{111} is shown below together with values derived from the same theoretical sources *A*, *B*, *C*, *D*, as listed in Table 2(*a*),

Molière & Wagenfeld 1·94 volt,

A: 1·25 volt, *B*: 1·46 volt, *C*: 1·62 volt, *D*: 1·99 volt.

As for V_{200}, an appreciable difference exists between the different calculations, and experimental evidence gives further support to Tokonami's result, *D*.

II. V_h^i *determination*

Comparison with other experimental results

The phenomenon of anomalous absorption with electrons was first observed quantitatively in the fine-structure diffraction from magnesium oxide (Honjo & Mihama, 1954) and directly in the central beam image of the Hillier pattern from molybdenite (Kohra & Watanabe, 1959), and since then the Fourier coefficients of absorption (V_h^i) have been estimated, by measurements on the magnesium oxide fine-structure (Lehmpfuhl & Molière, 1962) and by two types of experiment in the electron microscope. Firstly Hashimoto, Howie & Whelan, in several experiments principally with aluminum observed the extinction contours occurring across images of bent single crystals in directions of constant thickness. The principle of this experiment is the same as that of the convergent beam method, the curvature of the crystal replacing the convergent beam as a means of obtaining diffraction over angle. However these experiments were not suitable for quantitative measurement.

On the other hand several investigations have been made based on the observation of pendellösung fringes in the image of magnesium oxide 90° wedge crystals. The method of analysis developed by Kohra & Watanabe (1961) using the bright-field image, and later by Watanabe, Fukuhara & Kohra (1962) using the dark field image, depends upon the observation of the 'amplitude curve' and the 'centre curve' of the image, corresponding to the envelope of the pendellösung fringes, and their mean value. Using the two-beam approximation the authors obtained a theoretical expression for the 'centre curve' subsequently referred to as the (W–F–K) expression, containing the factor $\cosh(V_h^i . T \ldots)$ where T is the crystal thickness.

The results obtained by this latter method, and specifically the measurements of V_{200}^i, have shown a

* In the present discussion the Mott scattering formula has been used in the conversion from electron density (F_x) and values shown in Table 2(*a*) contain this approximation. The accuracy of this formula when applied to negative ions, such as O^{2-} is the subject of current investigation, which will be reported separately.

wide divergence not only from the (W–F–K) theoretical relation but also from one measurement to another. The average value from these experiments is considerably higher than that obtained in the present experiment and other electron diffraction measurements (*e.g.* Table 3). A summary of the apparent disagreements is given by Kamiya (1963). The above authors and also Uyeda & Nonoyama (1965) have stressed the importance of the inelastically scattered electrons to the resulting intensity distribution. Further consideration shows in addition other important factors. For the electron microscope it is also necessary to consider the conditions of illumination, and the effects of coherent diffuse scattering. These effects become further complicated when a wedge crystal is used. These factors, together with the use of the two-beam approximation, provide a satisfactory explanation of the different results obtained.

Table 3. *Experimental and theoretical values of* V'_{200} *in volts for magnesium oxide*

Watanabe, Fukuhara & Kohra	0·82 (100 kV)
Kamiya	0·6 (50 kV)
Lehmpfuhl*	0·16 (57 kV)
Present experiment	0·14 (80 kV)
Present experiment, with two-beam interpretation	0·3 (80 kV)
Yoshioka & Kainuma	0·6 (40 kV)
Yoshioka & Kainuma	0·36 (corrected for 80 kV)

* Unpublished result, from diffraction fine-structure measurements, using a wedge crystal.

1. *n-Beam effects.* Use of the two-beam formulation for interpretation has been found in the present analysis to lead to an error of 100% in the estimate for V'_h for the 200 case, as compared with an error of 10% in the V_h estimate. The result for 80 kV with the two-beam method is $V'_{200}=0{\cdot}3$ volt compared with 0·14 volt from the *n*-beam analysis. The relatively greater importance of *n*-beam effects in the case of absorption scattering can be seen in the correspondingly slow angular fall-off found for the absorption scattering factors. The effect of the systematic interaction becomes most pronounced when the excitation error, ζ, of the main reflexion is non-zero. Kamiya's results for V'_{200}, obtained by two-beam calculation for cases of large ζ* clearly show this influence. Uyeda & Nonoyama found no agreement with the calculated (W–F–K) intensities even for $\zeta=0$, and concluded that the complex potential method of describing the Borrmann effect was invalid. However, experiments employing parallel-sided crystals and using *n*-beam theory have shown good agreement with this method (provided the V'_h term is accepted as a function of the experiment, unlike V_h).

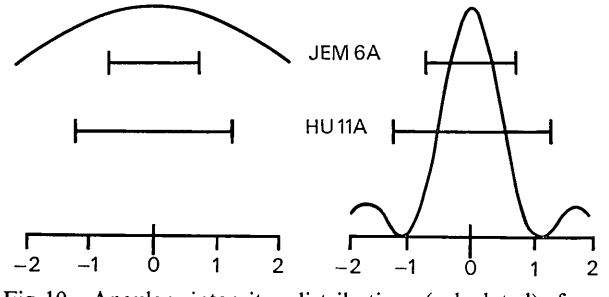

Fig. 10. Angular intensity distribution (calculated) for a magnesium oxide crystal of thickness $N=2$, and $N=10$, where N corresponds to the pendellösung fringe number in the wedge-crystal experiment, and the crystal thickness $T=(N-\frac{1}{2})l_{200}$, where $l_{200}=408$ Å. Units of the abscissa are 10^{-3} radian.

2. *Angular aperture of illumination at the specimen.* In the electron microscope the source is normally focused near the specimen by the second condenser lens, in order to give sufficient illumination. Under these conditions the angular spread in the radiation falling on the specimen, which would be further increased by the objective lens fore-field, is of the same order as the width of the diffraction maxima arising from the thicker regions of the crystal, *i.e.* $\sim 10^{-3}$ radian. Fig. 10 shows two angular diffraction distributions from crystal thicknesses which correspond to the local thickness at the second and the tenth bright pendellösung fringe of a magnesium oxide wedge, set at the 200 position. Also shown is the angular illuminating aperture from which the image is formed, for the HU-11A and JEM-6A microscopes when the 300 μ condenser aperture is used. It is seen that for the fringe number $N=2$ only the central region of the maximum is used, whereas for $N=10$ the region to the first minima is included. The main result to be expected in the image is that an additional damping of the pendellösung fringes will occur at high N values, with a consequent change in the measured absorption effect.

3. *Inelastic scattering: thickness dependence.* The possible influence of inelastic scattering, *i.e.* scattering processes in which the electron suffers a finite energy loss other than thermal losses, on the microscope pendellösung measurements was pointed out by Uyeda (1962) and by Watanabe *et al.* (1962), and the effect was shown experimentally by Kamiya (1963) to be important. However it does not necessarily have the same importance in other experiments. The effect may be shown to have a thickness dependence, by means of an argument due to Cowley and employed by Kuwabara (1966). For the sake of clarity we give this argument here in detail.

When an electron suffers an energy loss ΔE somewhere in the crystal there are two effects. Firstly a wavelength change results, and secondly the electron loses coherence relative to other electrons from the same part of the source. The first effect, resulting in a small change in the diffraction angles will be experimentally undetectable. The second effect is the one which has been considered important in dynamic scat-

* The relation between the excitation error ζ and W used in the above references is $\zeta=W(4\pi m\lambda V_h/h^2)$, with V_h in volts.

tering. It is useful to connect ΔE with D, the smallest crystal region in which the energy transfer can be localized. D is a distance measured in the electron beam direction, and D and ΔE are related by Heisenberg's uncertainty principle. When D is greater than the crystal thickness T, an electron suffering the loss ΔE behaves dynamically exactly as other no-loss electrons, and will give the same Borrmann coefficient. When D is smaller than T the energy loss can to some extent be localized in the crystal, and the loss electrons will give a dynamic diffraction pattern from a coherent depth less than the crystal thickness. Further, the resulting intensity will be given by averaging those patterns arising from thicknesses in the range D to T (Kuwabara, 1966).

For the wedge experiment the effective thickness corresponding to the 'centre curve' for coherent inelastically scattered electrons (*i.e.* D above) becomes progressively less than the actual crystal thickness (T) after a certain point, and in addition the averaging effect reduces the structure in the curve at higher fringe numbers. These effects can be observed in Fig. 6(*a*) and Fig. 7 respectively of Kamiya's (1963) paper. The (W–F–K) formula will then give a lower value of V_h^i for the loss electrons, and it is necessary to filter the pattern and measure only the no-loss contribution.

For magnesium oxide the principal loss occurs for $\Delta E = 25$ eV (Watanabe, 1954) corresponding to a D value of ~ 240 Å. Inelastic scattering from thicker regions will progressively show a changed result. The degree of influence on the diffraction pattern will depend on the cross-section of the process, which itself is a function of accelerating voltage, and the actual thickness. In the present experiment no filter was used, but the convergent beam pattern itself offers a sensitive check of the presence of incoherent inelastic scattering. If we consider the effect of inelastic scattering on the intensity distributions analysed in the previous section, it is necessary to add to the calculated distributions the inelastic distributions corresponding to an averaged reduced thickness. In the strong beam, 000, 200, distributions, this added contribution would be difficult to detect owing to the relatively slow intensity oscillation (and would lower the values estimated for V_{200} and V_{200}^i by the two-beam formula, where these terms occur in product with T). On the other hand, the effect on the weak beam distribution of averaging over only a few unit cells is much more pronounced. From Fig. 4 it is seen that an averaged distribution for the 400 beam would soon loose its structure and become indistinguishable from the diffuse background. Since however, the rapid intensity oscillations from the experiment are accurately reproduced in the calculation we conclude that the inelastic background plays no important part in these measurements, even though the crystal thickness (650 Å) exceeds the coherence length for 25 eV. Presumably for thicker crystals (or lower accelerating voltages) the inelastic influence would become observable. The use of relatively thin crystals is desired for this reason. Also the general diffuse background, mostly from the strong beams, increases with thickness. A monotonic background was subtracted from the weak beam distributions prior to analysis.

4. *Imaging of coherent diffuse scattering.* According to recent theories (Yoshioka & Kainuma, 1962; Hall & Hirsch, 1965) anomalous absorption in electron diffraction can be explained by dynamic interactions in the thermal diffuse scattering. Normally only electrons occurring in the sharp Bragg reflexions are considered in the derivation as forming the image or pattern, which corresponds to the situation in the diffraction camera. In the microscope diffuse scattering within the objective aperture is recombined by the objective lens. The imaging properties of the diffuse scattering were investigated by Kamiya & Uyeda* (1961, 1962). They found that the experimental absorption coefficients V_h^i and V_0^i are dependent on the size of the objective

* Kamiya & Uyeda (also Uyeda, 1955) use the term *incoherent* to describe the diffuse scattering. Thermal diffuse scattering (T.D.S.) is generally treated theoretically as coherent with the Bragg scattering, which should hold except for very thick crystals. Other factors, however, are relevant in imaging diffuse scattering, since even with a perfect lens the interference pattern from a larger aperture may be beyond resolution. Images of pendellösung formed from apertures comparable in dimension to the diffraction fine-structure ($< 5\mu$) should be formed coherently, while from larger apertures, such as are controlled by normal objective apertures, they will be formed effectively by incoherent addition of T.D.S. pendellösung images. Both processes, though in different degrees, appear to increase the measured value V_h^i. If however an *incoherent source* of diffuse scattering is proposed, a decrease in the measured ratio V_h^i/V_0^i is expected when the aperture is increased, contrary to Hashimoto's observations.

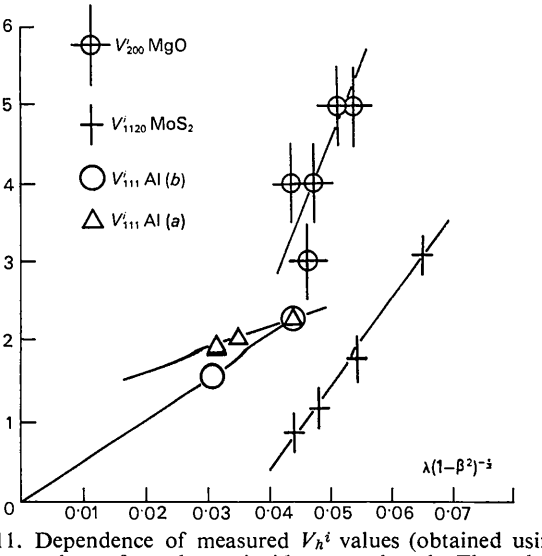

Fig. 11. Dependence of measured V_h^i values (obtained using the two-beam formula) on incident wavelength. The values for aluminum are from electron miscroscope investigation (Hashimoto, 1964) using (*a*) a fixed objective aperture and (*b*) an aperture approximately proportional to wavlength. The other values shown with crosses are obtained by convergent beam diffraction.

aperture. Hashimoto (1964), working with different accelerating voltages, and with different objective apertures, found that the anomalous absorption is increased by increasing the objective aperture, and that the dependence of the absorption on accelerating voltage is affected by the diffuse scattering. From the above theories V_h^i is proportional to $\lambda(1-\beta^2)^{-\frac{1}{2}}$. Hashimoto's results showed that with a fixed aperture size V_h^i was almost independent of wavelength. When the aperture size was changed to correspond to a constant diffraction distance (a constant 'effective' aperture) the results showed better agreement with the theory (Fig. 11). However these results still contain recombined diffuse scattering, though from a constant region of reciprocal space.

In the convergent beam experiment the diffuse scattering is not coherently imaged in this way, but is responsible for adding a diffused background to the sharp diffraction discs. This contribution is observable just outside the sharp discs and has a certain structure, generally differing from that of the sharp pattern. Its influence on the measurement appears to be small for thin crystals, but is expected to increase if the thickness or wavelength is much increased, owing to the increased cross-section and also increased diffuse spread relative to the pattern. Future investigations may require analysis of the diffuse region.

No investigation of behaviour with changing accelerating voltage has been made in this present work. However results already available from convergent beam investigations sufficiently establish this behaviour. Results obtained for MgO (V_{200}^i) (Lehmpfuhl, 1966) and MoS_2 ($V_{11\bar{2}0}^i$) (Goodman & Lehmpfuhl, 1965) with the use of the two-beam approximation are plotted against $\lambda(1-\beta^2)^{-\frac{1}{2}}$ in Fig. 11, together with the electron microscope results obtained by the same approximation. The points show a much steeper dependence on wavelength than either of the electron microscope results. The curves do not pass through the origin as expected from the above (two-beam) theories. For a more detailed understanding it will be necessary to examine the wavelength dependence by the n-beam method, knowing also the diffuse contribution.

Summary

The discrepancy between reported values of V_{200}^i measured in the microscope and in the diffraction camera has two apparent main causes. Firstly the application of the two-beam approximation has not been justified, and leads to high values of V_h^i. In addition, particularly with n-beam interactions, it is necessary to determine the excitation errors with some precision. This presents a difficulty in the electron microscope experiment. Results obtained without regard to sign and value of the excitation error will show a wide spread.

Secondly the inclusion of diffuse scattering in the image, a basic property of the electron microscope, has been found to increase the value obtained for V_h^i, and to change the nature of its dependence on accelerating voltage.

Further, inelastic scattering will influence the results obtained for thick crystals or wedge crystals, and the electron microscope illumination geometry will also affect the results in these cases.

From these considerations the diffraction camera results should be more suitable for comparison with theory.

Comparison with theory

The δ function character of the absorption potential found here for magnesium oxide at near room temperature is to be contrasted with the conclusions of Howie & Whelan for aluminum. From visual estimation of the bright-field image contrast they concluded that the absorption centres were less localized. This difference may arise from the corresponding Debye temperatures of magnesium oxide and aluminum, namely 800 °C and 390 °C respectively. However further work over a range of temperatures is needed to examine this temperature dependence.

Because of the limited degree of interaction for the magnesium oxide systematics, the V_h^i values could not be refined further. The accuracy of this measurement also may be restricted by the systematic approximation, to a greater degree than the V_h measurement, and this error must be further investigated. An independent determination of V_{420}, using in this case the two-beam approximation, gave a further value for comparison, of $\sim 0{\cdot}12$ volt.

Experimental and theoretical V_{200}^i values are shown in Table 3. The microscope values are higher than those from diffraction experiments. The theory based on thermal diffuse scattering alone gives the right magnitude for absorption: the result from Yoshioka & Kainuma* is in approximate agreement with our experiment interpreted by the two-beam method. However, present theories have been based on the two-beam approximation, and make approximations for the phonon model. It would seem necessary to include n-beam interactions in the theory, together with an appropriate multi-phonon distribution, before detailed agreement can be expected with experiment.

The authors wish to thank Dr V. Maslen for showing us the theoretical work on the O^{2-} ion, and to Mr A. F. Moodie for assistance given throughout the project. In addition one of us (G. Lehmpfuhl) wishes to thank the C.S.I.R.O. Division of Chemical Physics (Melbourne) and the Fritz-Haber-Institut (Berlin) for financing study leave.

* It is not meant to imply that the theory of Yoshioka & Kainuma, which is in itself quite general, contains a two-beam approximation. However, the only numerical calculation available to us is one made for the two-beam case for the MgO 200 reflexion, which was presented at a symposium in Tokyo in 1959. This result is given in Table 3.

References

ACKERMANN, I. (1948*a*). *Ann. der Physik*, **2**, 19.
ACKERMANN, I. (1948*b*). *Ann. der Physik*, **2**, 41.
BURLEY, G. (1965). *J. Phys. Chem. Solids*, **26**, 1605.
COCKAYNE, D. J. H., GOODMAN, P., MILLS, J. C. & MOODIE, A. F. (1966). To be published.
COWLEY, J. M., GOODMAN, P. & REES, A. L. G. (1957). *Acta Cryst.* **10**, 19.
COWLEY, J. M. & MOODIE, A. F. (1957). *Proc. Phys. Soc.* **71**, 533.
DUPOUY, G., PERRIER, F., UYEDA, R. & AYROLES, R. (1965). *J. Microscopie*, **4**, 429.
FUJIWARA, K. (1961). *J. Phys. Soc. Japan*, **16**, 2226.
GJØNNES, J. (1962). *Acta Cryst.* **12**, 412.
GOODMAN, P. & LEHMPFUHL, G. (1965). *Z. Naturforsch.* **20**a, 110.
GOODMAN, P. & LEHMPFUHL, G. (1966). *Acta Cryst.* Submitted for publication.
GOODMAN, P. & MOODIE, A. F. (1966). To be published.
HALL, C. R. & HIRSCH, F. R. S. (1965). *Proc. Roy. Soc.* A**286**, 158.
HASHIMOTO, H. (1964). *J. Appl. Phys.* **35**, 277.
HASHIMOTO, H., HOWIE, A. & WHELAN, M. J. (1962). *Proc. Roy. Soc.* A**269**, 80.
HATTORI, H., KURIYAMA, H., KATAGAWA, T. & KATO, N. (1965). *J. Phys. Soc. Japan*, **20**, 988.
HONJO, G. & MIHAMA, K. (1954). *J. Phys. Soc. Japan*, **9**, 184.
HOWIE, A. & WHELAN, M. J. (1960). *Proc. European Regional Conf. Electron Microscopy, Delft*, p.181.
KAMIYA, Y. (1963). *Japan J. Appl. Phys.* **2**, 386.
KAMIYA, Y. & UYEDA, R. (1961). *J. Phys. Soc. Japan*, **16**, 1361.
KAMIYA, Y. & UYEDA, R. (1962). *J. Phys. Soc. Japan.* **17**, B-II, p. 000.
KOHRA, K. & WATANABE, H. (1959). *J. Phys. Soc. Japan*, **14**, 1119.
KOSSEL, W. & MÖLLENSTEDT, G. (1939). *Ann. Phys., Lpz.* **5**, 113.
KUWABARA, S. (1966). *J. Phys. Soc. Japan*, **21**, 127.
LEHMPFUHL, G. (1966). Unpublished work.
LEHMPFUHL, G. & MOLIÈRE, K. (1961). *Z. Phys.* **164**, 398.
LEHMPFUHL, G. & MOLIÈRE, K. (1962). *J. Phys. Soc. Japan*, **17**, B-II, 130.
MACGILLAVRY, C. H. (1940). *Physica*, **7**, 329.
MIYAKE, S., FUJIWARA, K. & SUZUKI, K. (1963). *J. Phys. Soc. Japan*, **18**, 1306.
MOLIÈRE, K. & NIEHRS, H. (1955). *Z. Phys.* **140**, 581.
MOLIÈRE, K. & WAGENFELD, H. (1957). *Z. Kristallogr.* **110**, 175.
SUZUKI, T. (1960). *Acta Cryst.* **13**, 279.
TOGAWA, S. (1964). *J. Phys. Soc. Japan*, **20**, 742.
TOKONAMI, M. (1966). To be published.
UYEDA, R. (1955). *J. Phys. Soc. Japan*, **10**, 256.
UYEDA, R. & NONOYAMA, M. (1965). *Jap. J. Appl. Phys.* **4**, 498.
WAGENFELD, H. (1958). Doctorate Thesis, Berlin Free University.
WATANABE, H. (1954). *Phys. Rev.* **95**, 1684.
WATANABE, M., FUKUHARA, A. & KOHRA, K. (1962). *J. Phys. Soc. Japan*, **17**, B-II, 1962.
WATSON, R. E. (1958). *Phys. Rev.* **111**, 1108.
YAMASHITA, J. & KOJIMA, M. (1952). *J. Phys. Soc. Japan*, **7**, 261.
YOSHIOKA, H. & KAINUMA, Y. (1962). *J. Phys. Soc. Japan*, **17**, B-II, 134.

Acta Cryst. (1967). **22**, 24

Anomalous Scattering and the Phase Problem

BY A. HERZENBERG AND H. S. M. LAU

Theoretical Physics Department, University of Manchester, England

(*Received* 30 *December* 1965)

The ambiguity of the phase obtained from the interference of normal and anomalous X-ray scattering by the method of 'Bijvoet pairs' with monochromatic X-rays can be resolved if diffraction is measured at several frequencies in the region of anomalous scattering. It is pointed out that for the anomalous region at the *K* edge of many atoms, a set of frequencies of just the right order of spread and spacing is provided by the characteristic *L* multiplet of an atom higher up the periodic table, so that all the information needed could be obtained in a single experiment if the *L* radiation could be produced. (A considerable white background could be tolerated.) Rough estimates suggest that for a unit cell containing a single anomalous scatterer, measurements of intensity with an accuracy of 1 % should suffice to solve an organic structure containing 100 atoms. The method should be applicable to the crystallography of proteins containing sulphur atoms, where the sulphur *K* edge may be studied with Mo *L* radiation. A numerical example is discussed.

1. Introduction

The use of the interference between normal and anomalous scattering of X-rays in the determination of phases is well known. A difficulty of the method is that a unique solution for the structure factors cannot be obtained with certainty from a single experiment with monochromatic X-rays, but only if the information so obtained is supplemented in some other way, for example by using a second frequency (Okaya & Pepinsky, 1961; Ramaseshan, 1964). All the information necessary could be obtained in a single experiment if one